

LINEAR MODELLING AND IDENTIFICATION OF A MOBILE ROBOT WITH DIFFERENTIAL DRIVE

Patrícia N. GUERRA* Pablo J. ALSINA* Adelardo A. D. MEDEIROS* Antônio P. ARAÚJO*
Federal University of Rio Grande do Norte – Department of Computer Engineering and Automation
UFRN-CT-DCA – Campus Universitário – 59072-970 Natal RN Brazil
patricia,adelardo,pablo,tinhojr@dca.ufrn.br

Keywords: Nonholonomic robots, robot control, stabilization control, linear modeling of robots.

Abstract: This paper presents a modelling and identification method for a wheeled mobile robot, including the actuator dynamics. Instead of the classic modelling approach, where the robot position coordinates (x, y) are utilized as state variables (resulting in a non linear model), the proposed discrete model is based on the travelled distance increment Δl . Thus, the resulting model is linear and time invariant and it can be identified through classical methods such as Recursive Least Mean Squares. This approach has a problem: Δl can not directly measured. In this paper, this problem is solved using an estimate $\widetilde{\Delta l}$ based on a second order curve approximation. Experimental data were collected and the proposed method was used to identify the model of a real robot.

1 Introduction

Usually, realistic mathematical models of mobile robots are obtained through the physics laws that govern their behavior. Approaches applying artificial intelligence techniques to the input and output measurements are also utilized. Several model types were developed for non holonomic mobile robots. LTI (*linear time invariant*) models are usually obtained through Taylor series linearization on only one point of operation of the system. A QLPV (*quasi-linear parameter-varying*) model for a car-like robot is presented in the literature (Economou et al., 2002).

The classic mathematical model of a mobile robot has a structure similar to the mathematical model of robot manipulators, so that techniques of parametric identification developed for the latter can be adapted for the former. However, most of these techniques assume that robot speed and acceleration measurements are available, which is not generally true.

Differently of the identification techniques for manipulators, enough discussed in the literature (Poignet and Gautier, 2000; Efe et al., 1999), the mobile robot identification techniques have been less studied. An identification of the dynamic model of a micro-robot using the recursive least mean square

method (RLMS) is presented by Pereira (Pereira, 2000; Pereira et al., 2000). As the model to be identified through RLMS is non linear, a simplification is used: the orientation $\theta(t)$, which is time-variant, is considered constant during each sampling period.

In this work a linear (not a linearized one) dynamic model for mobile robots is presented. The proposed model is equivalent to the non linear dynamic model, commonly adopted for non-holonomic mobile robots (Yamamoto et al., 2003). The proposed model uses the variable Δl , distance traveled by the robot during a sampling interval, instead of the traditional modelling, where its absolute position is used (x, y) . The problem due to the impossibility of measuring the traveled distance Δl during a sampling period is overcome through the use of an estimate, $\widetilde{\Delta l}$, of this value. The identification of this discrete dynamic model is attained using a classic method of identification of linear systems, the recursive least mean squares.

The rest of this paper is organized as follows. Section 2 describes the robot and its modelling by the equivalent linear and non-linear models. Section 3 presents the proposed calculation method for a numeric value of the immeasurable variable Δl . In section 4, experimental results validating the proposed approach are shown. Finally, in section 5, the obtained results are discussed and the conclusions and future perspectives are presented.

¹The authors received partial financial support of the Brazilian agencies CAPES and CNPq.

2 Robot Modelling

Figure 1 presents a diagram of the kind of robot we consider in this work. The robot has two wheels, driven by two independent electric motors. The wheels are placed at each side of the robot, in such a position that their rotation axis are coincident. The robot configuration is represented by the position of the center of the axis between the two wheels in the Cartesian space (x and y) and by its orientation θ (angle between the vector of the robot orientation and the abscissas axis).

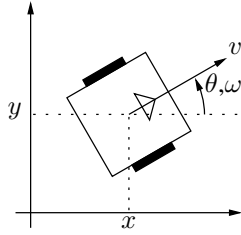


Figure 1: Robot modelling

2.1 Cinematic Model

The cinematic model describes the relations between the derivatives of robot position and orientation and the robot linear and angular speeds, v and w , without taking into account the causes of its movement:

$$\begin{bmatrix} \dot{x} \\ \dot{y} \\ \dot{\theta} \end{bmatrix} = \begin{bmatrix} \cos \theta & 0 \\ \sin \theta & 0 \\ 0 & 1 \end{bmatrix} \cdot \begin{bmatrix} v \\ w \end{bmatrix} \quad (1)$$

This equation models the non-holonomic restrictions of the robot, due to the fact of its wheels not allowing lateral movements.

2.2 Dynamic Model

The dynamic model is derived from the physics laws that govern the several robot subsystems, including the actuator dynamics (electric and mechanical characteristics of the motors), friction and robot dynamics (movement equations). The derivation of this model for a small mobile robot (Vieira et al., 2001) was presented by Yamamoto (Yamamoto et al., 2003).

For most robots, the modelling process generates a second-order model expressed by equation 2:

$$\mathbf{K}\mathbf{u} = \mathbf{M}\dot{\mathbf{v}} + \mathbf{B}\mathbf{v} \quad (2)$$

where $\mathbf{v} = [v \ w]^T$ represents the robot linear and angular speeds, $\mathbf{u} = [e_r \ e_l]^T$ contains the input signals (usually armature tensions) applied to the right

and left motors, \mathbf{K} is the matrix which transforms the electrical signals \mathbf{u} into forces to be generated by the robot wheels, \mathbf{M} is the generalized inertia matrix and \mathbf{B} is the generalized damping matrix, which includes terms of viscous friction and electric resistance.

2.3 Equivalent Linear Model

The complete robot model, obtained from the union of equations 1 and 2, can be represented by the following state equation:

$$\begin{bmatrix} \dot{v} \\ \dot{\omega} \\ \dot{x} \\ \dot{y} \\ \dot{\theta} \end{bmatrix} = \begin{bmatrix} -\mathbf{M}^{-1}\mathbf{B} & \vdots & \mathbf{0} \\ \dots & \dots & \dots \\ \cos(\theta) & 0 & \vdots \\ \sin(\theta) & 0 & \vdots \\ 0 & 1 & \vdots \end{bmatrix} \begin{bmatrix} v \\ \omega \\ x \\ y \\ \theta \end{bmatrix} + \begin{bmatrix} \mathbf{M}^{-1}\mathbf{K} \\ \dots \\ \mathbf{0} \end{bmatrix} \begin{bmatrix} e_r \\ e_l \end{bmatrix} \quad (3)$$

$$\mathbf{y} = \begin{bmatrix} 0 & 0 & 1 & 0 & 0 \\ 0 & 0 & 0 & 1 & 0 \\ 0 & 0 & 0 & 0 & 1 \end{bmatrix} \begin{bmatrix} v \\ \omega \\ x \\ y \\ \theta \end{bmatrix}$$

where the system output $\mathbf{y} = [x \ y \ \theta]^T$ corresponds to the robot configuration.

To allow the application of linear discretization techniques, we will rewrite the system equations into a linear representation of the robot dynamic behavior. To attain this objective, we need to change the set of state variables: the robot's configuration, given by its position x and y and its orientation θ , will be described in terms of the robot linear displacement l and the robot orientation θ .

$$\begin{bmatrix} \dot{v} \\ \dot{\omega} \\ \dot{l} \\ \dot{\theta} \end{bmatrix} = \begin{bmatrix} -\mathbf{M}^{-1}\mathbf{B} & \vdots & \mathbf{0} \\ \dots & \dots & \dots \\ 1 & 0 & \vdots \\ 0 & 1 & \vdots \end{bmatrix} \begin{bmatrix} v \\ \omega \\ l \\ \theta \end{bmatrix} + \begin{bmatrix} \mathbf{M}^{-1}\mathbf{K} \\ \dots \\ \mathbf{0} \end{bmatrix} \begin{bmatrix} e_r \\ e_l \end{bmatrix} \quad (4)$$

$$\mathbf{z} = \begin{bmatrix} 0 & 0 & 1 & 0 \\ 0 & 0 & 0 & 1 \end{bmatrix} \begin{bmatrix} v \\ \omega \\ l \\ \theta \end{bmatrix}$$

The new state equation 4 has the same dynamic parameters than the original state equation 3 but a new system output $\mathbf{z} = [l \ \theta]^T$. We observe that the linear equivalent model was obtained without any simplification assumption. In this way, the linear model is an exact equivalent representation of the original non-linear representation in equation 3.

2.4 Model Discretization

To allow the application of the classical estimation techniques, it is necessary to derive a discrete transfer function equivalent to the model in equation 4. The first step is the transformation of the state space form into a continuous transfer matrix:

$$\begin{bmatrix} L(s) \\ \theta(s) \end{bmatrix} = \begin{bmatrix} G_{11}(s) & G_{12}(s) \\ G_{21}(s) & G_{22}(s) \end{bmatrix} \cdot \begin{bmatrix} E_r(s) \\ E_l(s) \end{bmatrix} \quad (5)$$

where each term $G_{ij}(s)$ has the following structure:

$$G_{ij}(s) = \frac{N_{ij}(s)}{D(s)} = \frac{\alpha_{ij}s + \beta_{ij}}{s(s^2 + k_1s + k_2)}$$

In the second step, we calculate the four discrete transfer functions $G_{ij}(z)$:

$$\begin{bmatrix} L(z) \\ \theta(z) \end{bmatrix} = \begin{bmatrix} G_{11}(z) & G_{12}(z) \\ G_{21}(z) & G_{22}(z) \end{bmatrix} \cdot \begin{bmatrix} E_r(z) \\ E_l(z) \end{bmatrix} \quad (6)$$

where each term $G_{ij}(z)$ has the following structure:

$$G_{ij}(z) = \frac{N_{ij}(z)}{D(z)} = \frac{\gamma_{ij}z^2 + \delta_{ij}z + \epsilon_{ij}}{(z-1)(z^2 + \alpha_1z + \alpha_2)}$$

To obtain a parametrisation appropriated to the parameter estimation, the transfer functions are converted to equivalent difference equations:

$$\Delta l_k = -\alpha_1 \Delta l_{k-1} - \alpha_2 \Delta l_{k-2} + \quad (7)$$

$$+ \gamma_{11}e_{r,k-1} + \delta_{11}e_{r,k-2} + \epsilon_{11}e_{r,k-3} + \gamma_{12}e_{l,k-1} + \delta_{12}e_{l,k-2} + \epsilon_{12}e_{l,k-3}$$

$$\Delta \theta_k = -\alpha_1 \Delta \theta_{k-1} - \alpha_2 \Delta \theta_{k-2} + \quad (8)$$

$$+ \gamma_{21}e_{r,k-1} + \delta_{21}e_{r,k-2} + \epsilon_{21}e_{r,k-3} + \gamma_{22}e_{l,k-1} + \delta_{22}e_{l,k-2} + \epsilon_{22}e_{l,k-3}$$

where $\Delta l_k = l_k - l_{k-1}$ is the linear distance traveled in a sampling period, $\Delta \theta_k = \theta_k - \theta_{k-1}$ is the angular increment in the robot's orientation in the same period, and $e_{r,k}$ and $e_{l,k}$ are the plant input signals.

3 Traveled Distance Computation

The variable Δl is not measurable. In spite of this, we can use heuristics to calculate a plausible value for this variable, $\widetilde{\Delta l}$. The methodology developed to calculate $\widetilde{\Delta l}$ consists of the following steps:

1. calculation of the path length $|\widetilde{\Delta l}|$
2. calculation of the direction of the movement, i.e. the sign of $\widetilde{\Delta l}$

3.1 Path Length Computation

It is possible to obtain with reasonable precision the robot configuration (x, y, θ) in two consecutive sampling instants, but we cannot be sure about the path traveled by the robot between the first configuration and the second configuration. However, a parametric curve $(x(\lambda), y(\lambda))$, $0 \leq \lambda \leq 1$ can be interpolated between these points and the length of this curve can be used as an estimated value of $|\widetilde{\Delta l}|$ (see figure 2).

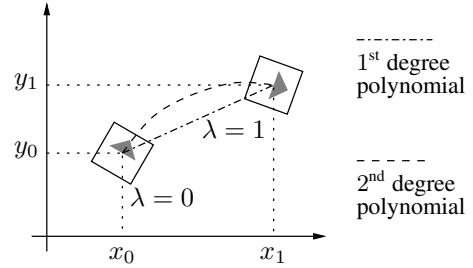


Figure 2: Diagram for $|\widetilde{\Delta l}|$ computation

Adopting a 1st order polynomial to interpolate, we are using the Euclidean distance as a measure of the length of the traveled distance. However, this solution violates the non-holonomic constraints of the system when the traveled path is not a straight line.

In this work, we used a parametric curve of 2nd degree to calculate the absolute value of $\widetilde{\Delta l}$ because this is the simplest polynomial allowing interpolating between the two configurations without violating the non-holonomics constrains at the contour conditions:

$$\begin{cases} x(\lambda) = a_2\lambda^2 + a_1\lambda + a_0 \\ y(\lambda) = b_2\lambda^2 + b_1\lambda + b_0 \\ \tan[\theta(\lambda)] = d(\lambda) = \frac{dy/d\lambda}{dx/d\lambda} = \frac{2b_2\lambda + b_1}{2a_2\lambda + a_1} \end{cases} \quad (9)$$

$$\begin{cases} x(0) = x_0 = a_0 \\ y(0) = y_0 = b_0 \\ x(1) = x_1 = a_2 + a_1 + a_0 \\ y(1) = y_1 = b_2 + b_1 + b_0 \\ d(0) = \tan(\theta_0) = \frac{b_1}{a_1} \\ d(1) = \tan(\theta_1) = \frac{2b_2 + b_1}{2a_2 + a_1} \end{cases} \quad (10)$$

Solving the system 10 results in the following general solution:

$$\begin{cases} a_0 = x_0 \\ a_1 = \frac{2[\tan(\theta_1)(x_1 - x_0) - y_1 + y_0]}{\tan(\theta_1) - \tan(\theta_0)} \\ a_2 = x_1 - x_0 - a_1 \\ b_0 = y_0 \\ b_1 = a_1 \tan(\theta_0) \\ b_2 = y_1 - y_0 - b_1 \end{cases} \quad (11)$$

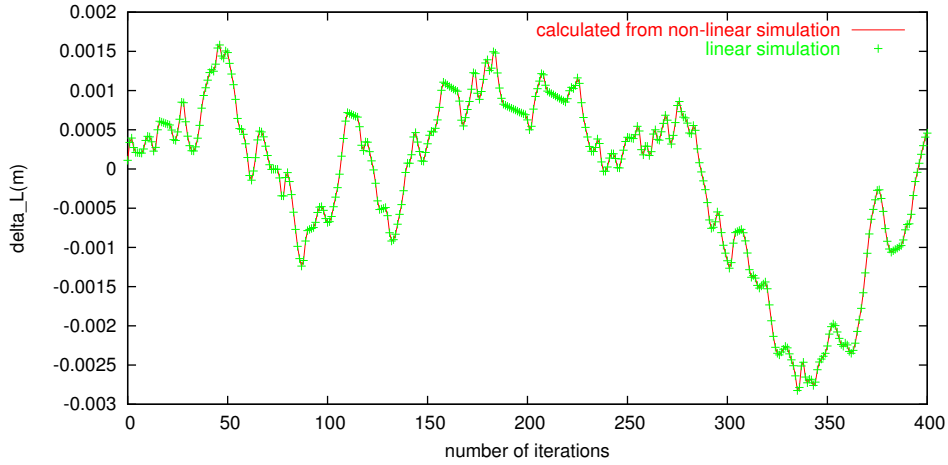


Figure 3: Comparison between $\widetilde{\Delta l}$ and Δl

Similar solutions can be found for the singular cases where θ_0 or θ_1 have values close to $\pm \frac{\pi}{2}$.

To calculate the length of this curve, we used:

$$|\widetilde{\Delta l}| = \int_0^1 \sqrt{\left(\frac{dx}{d\lambda}\right)^2 + \left(\frac{dy}{d\lambda}\right)^2} d\lambda \quad (12)$$

Substituting $\frac{dx}{d\lambda}$ and $\frac{dy}{d\lambda}$ in equation 12 we obtain:

$$|\widetilde{\Delta l}| = \int_0^1 \sqrt{A\lambda^2 + B\lambda + C} d\lambda \quad (13)$$

where

$$\begin{cases} A = 4a_2^2 + 4b_2^2 \\ B = 4a_1a_2 + 4b_1b_2 \\ C = a_1^2 + b_1^2 \end{cases} \quad (14)$$

The closed solution for the integral in equation 13 can be found in integral tables.

3.2 Computation of the Movement Direction

To obtain the sign of the traveled distance, i.e. knowing if the robot moved forward or backward, we calculate the value of 0x_1 , the x coordinate of the current configuration point (x_1, y_1) calculated with respect to the reference frame attached to the previous robot position (x_0, y_0) , as indicated in the figure 4. If 0x_1 is positive, the robot will have moved forward and $\widetilde{\Delta l} > 0$. Otherwise, the robot will have moved backward and $\widetilde{\Delta l} < 0$.

A simple coordinate transformation allows the calculation of 0x_1 :

$$\begin{aligned} {}^0x_1 = & x_1 \cos \theta_0 - x_0 \cos \theta_0 + \\ & + y_1 \sin \theta_0 - y_0 \sin \theta_0 \end{aligned} \quad (15)$$

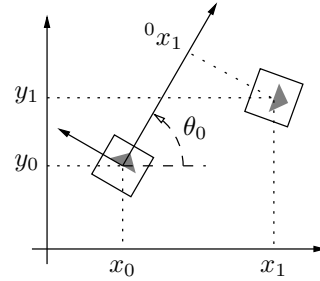


Figure 4: Diagram for calculating the sign of $\widetilde{\Delta l}$

3.3 Validation of Traveled Distance Computation

Several tests were performed to validate the approximation of Δl by $\widetilde{\Delta l}$. We simulated the linear system described by equation 4 and the non-linear system described by equation 3 with the same input values (e_r and e_l), obtaining as outputs, respectively:

$$\mathbf{z} = \begin{bmatrix} l \\ \theta \end{bmatrix} \quad \text{and} \quad \mathbf{y} = \begin{bmatrix} x \\ y \\ \theta \end{bmatrix}$$

After this, we plotted the values of $\Delta l = l_k - l_{k-1}$, generated by the linear system, and $\widetilde{\Delta l}$, which was calculated using the x and y outputs generated by the non-linear system and the proposed approximation. From figure 3, we can observe that $\widetilde{\Delta l}$ (estimated value) is very close to the actual distance traveled by the robot (Δl). The mean error was 0,058%, with a standard deviation of 0,274%.

4 Experimental results

The results presented in this section were obtained using a small ($7.5 \times 7.5 \times 7.5$ cm) mobile robot, with two wheels driven by two independent DC motors, very used in robot soccer competitions. A detailed description of the robot can be found in precedent articles (Vieira et al., 2001).

The inputs signals e_r and e_l are the armature voltages of the right and left DC motors. The system output $\mathbf{y} = [x \ y \ \theta]^T$ is measured by processing the image from a fixed camera placed over the robot workspace (Aires et al., 2001). We use a sampling rate of 30 samples per second, fixed by the image acquisition card.

The classical method of Recursive Least Mean Squares (Åström and Wittenmark, 1997) was utilized for the estimation of the parameters of the model (equations 7 and 8). The system was excited with pseudo-random input signals, assuming values between 1.0 (100% of the motor supply voltage, 9V) and -1.0 (-9V). As the robot has some high time constants, the input values only changed at each 8 sampling periods. To reduce the chance of high velocities, the tensions near 0.0 were more probable than the tensions near ± 1.0 .

Figure 9 shows the trajectory followed by the robot during an experiment with 500 samples. The resulting estimated parameters are presented in table 1.

	$\alpha_1 = -0.2125$		$\alpha_2 = -0.5362$
i,j	γ_{ij}	δ_{ij}	ϵ_{ij}
11	-0.0005195	-0.0005098	0.003019
12	-0.0001753	-0.001158	0.003347
21	0.01099	-0.02627	-0.03326
22	0.001818	-0.06038	0.1074

Table 1: Estimated parameters

Figure 5 shows the measured and estimated values for $\Delta\theta$. The error in the estimation of $\Delta\theta$ has mean value of 0.000426rad and standard deviation of 0.0685rad. Figure 6 shows the calculated values of $\widetilde{\Delta l}$ and the estimated values for Δl . The error in the estimation of Δl has mean value of -0.000297m and standard deviation of 0.00261m.

To validate the generality of the obtained model, we calculate the estimation errors using the same parameters with a different trajectory (figure 10). Figure 7 shows the measured and estimated values for $\Delta\theta$ (mean value of 0.00878rad and standard deviation of 0.0814rad) and figure 8 shows the calculated values of $\widetilde{\Delta l}$ and the estimated values for Δl (mean value of -0.000435m and standard deviation of 0.00267m).

5 Conclusion

We proposed the substitution of the robot position variables (x, y) by the distance traveled in a sampling period Δl . This substitution resulted in an equivalent exact linear dynamic model, suitable for identification through the standard linear systems methods. Moreover, the linearity of the proposed model allows its application on the design of dynamic controllers based on classic linear discrete techniques, as proposed by Vieira et al., (2004).

It can be observed that, in spite of the fact that the identified model have been defined in the discrete domain, there is no impediment of obtaining the continuous model from the same, also allowing its use in the design of controllers in the continuous domain.

REFERENCES

- Aires, K. R. T., Alsina, P. J., and Medeiros, A. A. D. (2001). A global vision system for mobile mini-robots. In *SBAI - Simpósio Brasileiro de Automação Inteligente*, Canela, RS, Brasil.
- Åström, K. J. and Wittenmark, B. (1997). *Computer Controlled Systems*. Information and System Sciences. Prentice-Hall, EUA, 3 edition. ISBN 0-13-314899-8.
- Economou, J., Tsourdos, A., and White, B. (2002). Takagi-sugeno model synthesis of a quasi-linear parameter varying mobile robot. In *IROS - IEEE/RSJ International Conference on Intelligent Robots and Systems*, volume 3, pages 2103–2108.
- Efe, M., Kaynak, O., and Rudas, I. (1999). A novel computationally intelligent architecture for identification and control of nonlinear systems. In *ICRA - IEEE International Conference on Robotics and Automation*, volume 3, pages 2073–2077, Detroit, MI, USA.
- Pereira, G. A. S. (2000). Identificação e controle de micro-robôs móveis. Master's thesis, Universidade Federal de Minas Gerais, Belo Horizonte, MG, Brazil.
- Pereira, G. A. S., Campos, M. F. M., and Aguirres, L. A. (2000). Modelo dinâmico para predição da posição e orientação de micro-robôs móveis observados por visão computacional. In *CBA - Congresso Brasileiro de Automática*, Florianópolis, SC, Brazil.
- Poignet, P. and Gautier, M. (2000). Comparison of weighted least squares and extended kalman filtering methods for dynamic identification of robots. In *ICRA - IEEE International Conference on Robotics and Automation*, volume 4, pages 3622–3627, San Francisco, CA, USA.
- Vieira, F. C., Alsina, P. J., and Medeiros, A. A. D. (2001). Micro-robot soccer team - mechanical and hardware implementation. In *Congresso Brasileiro de Engenharia Mecânica*, pages 534–540.

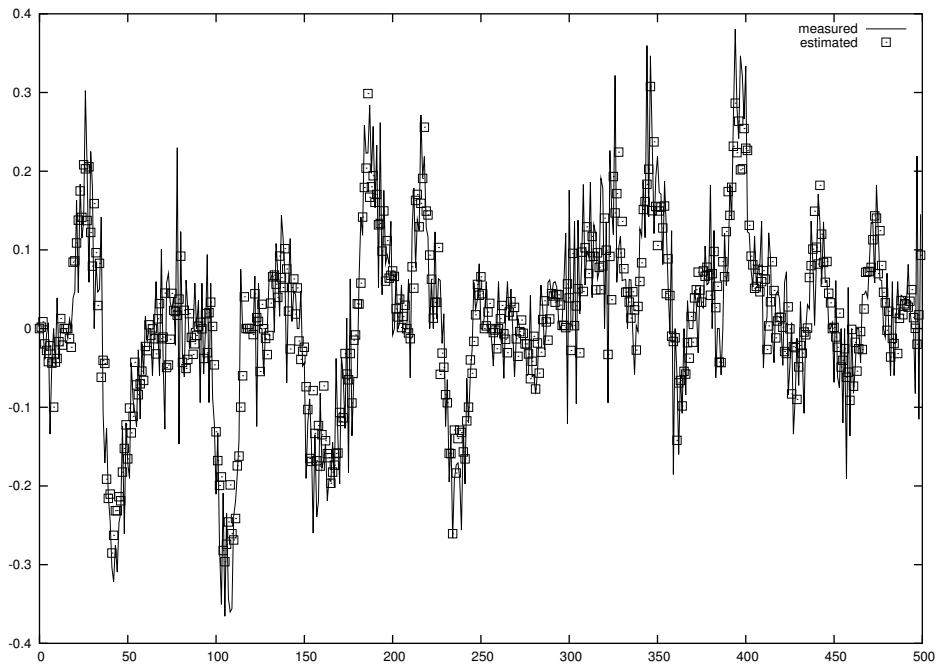


Figure 5: $\Delta\theta$ measured and $\Delta\theta$ estimated

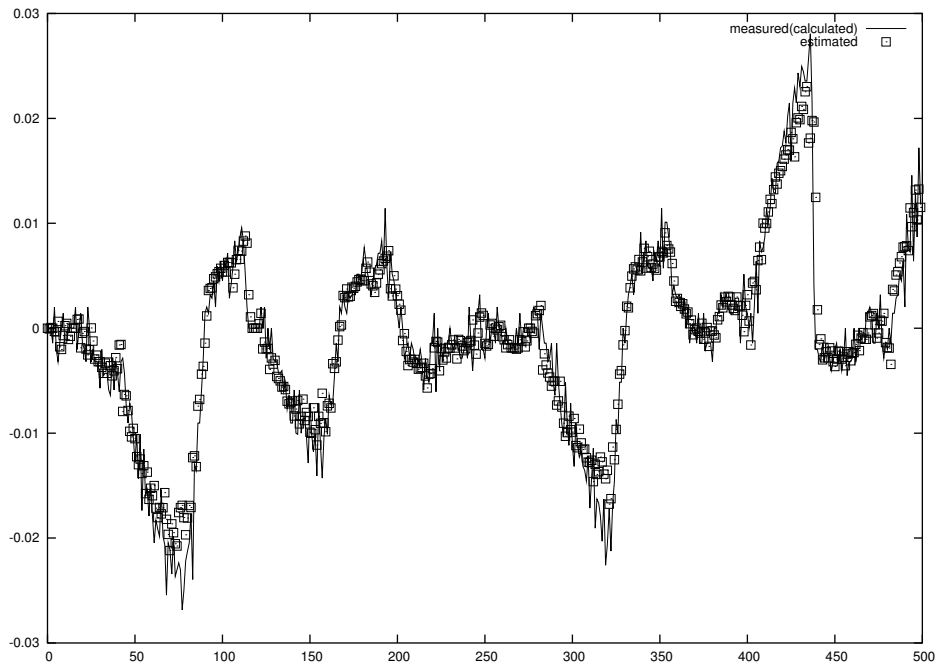


Figure 6: $\widetilde{\Delta l}$ calculated and Δl estimated

Vieira, F. C., Medeiros, A. A. D., Alsina, P. J., and Araújo Jr., A. P. (2004). Position and orientation control of a two-wheeled differentially driven nonholonomic mobile robot. In *ICINCO – International Con-*

ference on Informatics in Control, Automation and Robotics, Setúbal, Portugal.

Yamamoto, M. M., Pedrosa, D. P. F., and Medeiros, A. A. D. (2003). Um simulador dinâmico para mini-

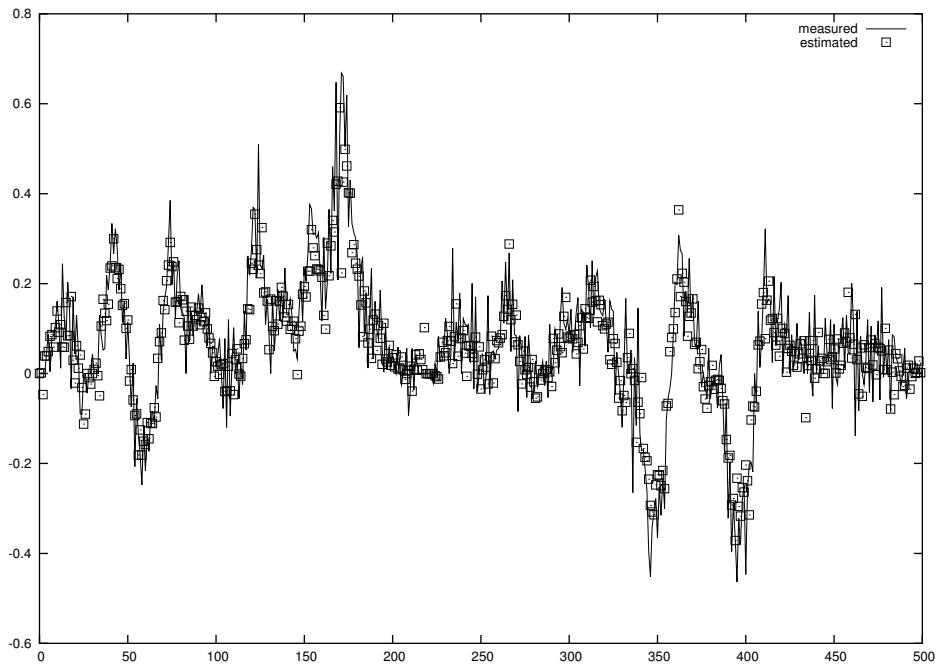


Figure 7: $\Delta\theta$ measured and $\Delta\theta$ estimated

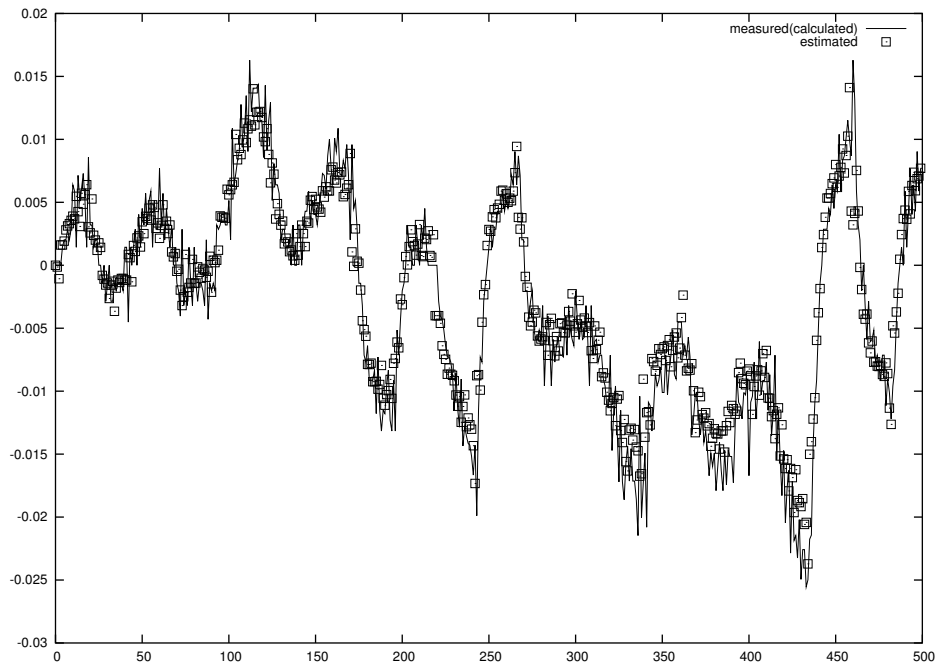


Figure 8: $\widetilde{\Delta l}$ calculated and Δl estimated

robôs móveis com modelagem de colisões. In *SBAI - Simpósio Brasileiro de Automação Inteligente*, Bauru, SP, Brazil.

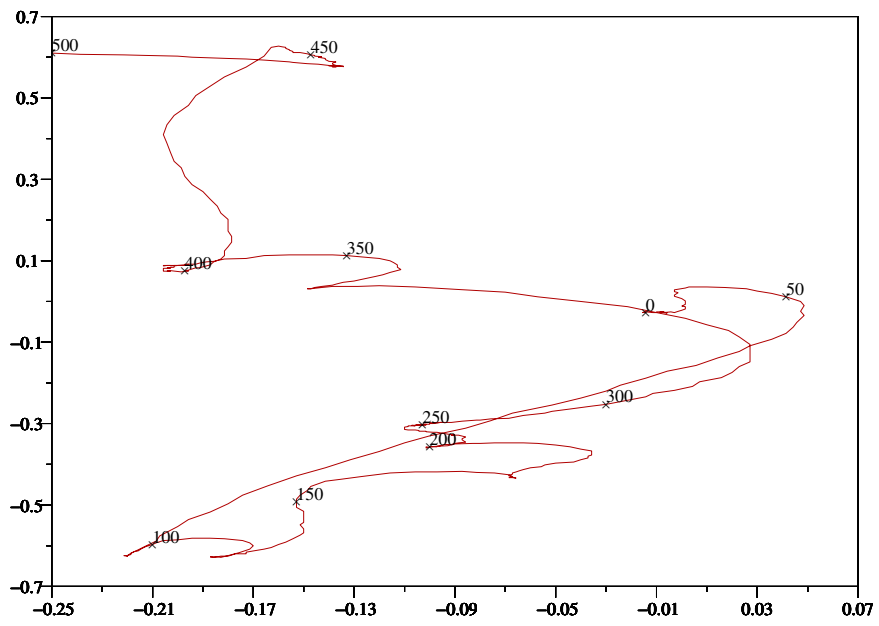


Figure 9: First example of system trajectory output

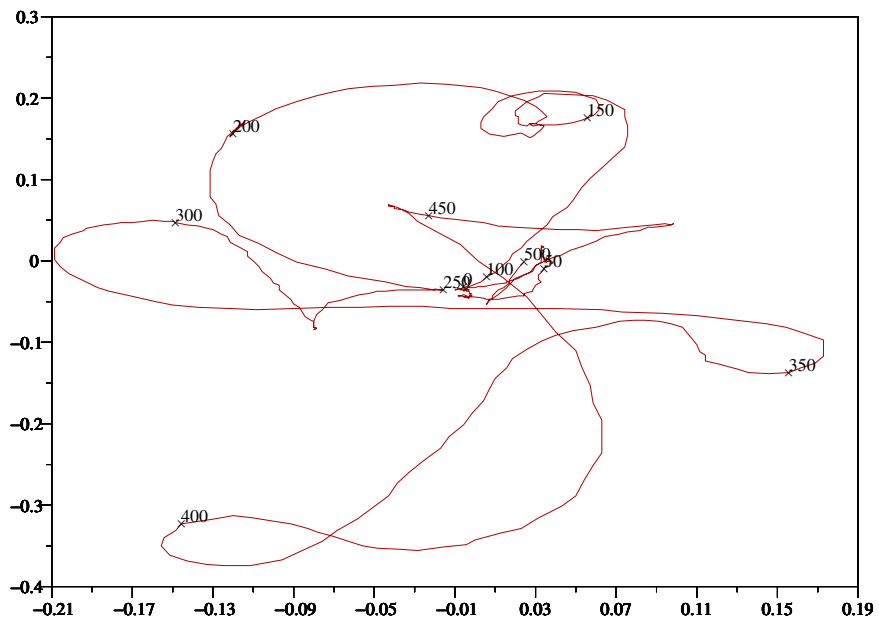


Figure 10: Second example of system trajectory output